Chemical Science

ROYAL SOCIETY OF CHEMISTRY

EDGE ARTICLE

View Article Online
View Journal | View Issue

Cite this: *Chem. Sci.*, 2023, **14**, 3938

All publication charges for this article have been paid for by the Royal Society of Chemistry

Bioinspired nucleobase-containing polyelectrolytes as robust and tunable adhesives by balancing the adhesive and cohesive properties†

Zhi Dong,[a] Jiang Wu,[a] Xinyi Shen,[a] Zan Hua *[b] and Guangming Liu *[a]

Supramolecular polymeric adhesives inspired by nature have been strongly pursued by scientists, since they possess strong but dynamic reversible adhesive behaviors concurrently. Optimizing the adhesive and cohesive properties is of vital importance for the fabrication of strong supramolecular polymeric adhesives, but common strategies often strengthen one property at the expense of another. Herein, counterion exchange of nucleobase-containing polyelectrolyte adhesives was utilized to boost the interfacial adhesion without compromising the intermolecular cohesion, achieving high adhesion strengths. By employing the cationic polyelectrolyte poly(3-acrylamidopropyltrimethylammonium chloride), the slightly enhanced intermolecular cohesion of the polyelectrolyte with hydrophobic sulfonates is capable of enhancing the adhesion strength. Intriguingly, by introducing bioinspired complementary nucleobases within adhesives, the loss of interfacial adhesion was observed for adhesives containing high supramolecular hydrogen-bonding crosslinking densities. By optimizing the cohesive and adhesive properties of nucleobase-containing polyelectrolyte adhesives using sulfonates with suitable chain lengths, 60 to 250 times improvement of adhesion strengths can be attained over that of initial supramolecular polymeric adhesives. Additionally, nucleobase-containing supramolecular polymeric adhesives tolerate different external conditions, maintaining robust adhesion strengths. This work offers us an efficient and feasible way to optimize the cohesive and adhesive properties for constructing robust and tunable supramolecular adhesives.

Received 8th February 2023
Accepted 14th March 2023

DOI: 10.1039/d3sc00697b

rsc.li/chemical-science

Introduction

Adhesives are essential and important for various applications involving industrial and medical products.[1–6] Based on the adhesive bonds, typical adhesives could be separated into three major categories. The first category of adhesives usually has strong adhesion strengths, depending on irreversible covalent bonds at the interface between the substrate and the adhesive. These adhesives include cyanoacrylates,[7] epoxy resins,[8,9] and so on. Although high adhesion strengths are obtained, the *in situ* formation of covalent bonds for efficient adhesion and cohesion often requires a long curing time. By contrast, the second kind of adhesives are capable of achieving relatively weak adhesion by employing reversible and non-covalent bonds based on the viscoelastic properties of polymers.[10–12] Their unique properties result in the wetting of the substrate with the hydrophobic interaction between the adhesive and the substrate, giving rise to fast and reversible adhesion. Inspired by nature, supramolecular polymeric adhesives have been intensely researched, which possess outstanding merits of both conventional adhesives.[13–17] They can bond to distinct substrates with high adhesion strength and good reversibility by combining multiple supramolecular interactions such as hydrogen bonds, metal-coordination bonds, π–π stacking, and hydrophobic interactions.[18–20]

Actually, catechol-based supramolecular adhesives have been widely developed after unraveling the molecular structures of adhesive proteins (Mfps-3 and 5) secreted by mussels.[21–27] Besides the catechol functionality, the cooperativity of catechols and positively charged amino acids in the adhesives is useful to improve the adhesion performance.[28–30] The cationic groups not only improve the interfacial adhesion by providing efficient surface binding, but also enhance cohesive properties by achieving the cation–π interactions.[28,31] Notably, the potential oxidation of catechol groups in the adhesives inevitably leads to the formation of covalent networks, damaging the reversible adhesive behaviors. Recently, nucleobases are also regarded as

[a]*Department of Chemical Physics, Key Laboratory of Surface and Interface Chemistry and Energy Catalysis of Anhui Higher Education Institutes, Hefei National Research Center for Physical Sciences at the Microscale, University of Science and Technology of China, Hefei, Anhui, 230026, China. E-mail: gml@ustc.edu.cn*

[b]*Biomass Molecular Engineering Center and Department of Materials Science and Engineering, Anhui Agricultural University, Hefei, Anhui, 230036, China. E-mail: z.hua@ahau.edu.cn*

† Electronic supplementary information (ESI) available: Synthetic details, ^{1}H NMR spectra, SEC traces, surface wettability, FT-IR spectra, XPS, and thermal and adhesive properties of nucleobase-containing polyelectrolytes with different counterions. See DOI: **https://doi.org/10.1039/d3sc00697b**

important moieties for fabricating robust supramolecular adhesives.[32–38] Similar to catechols, nucleobases especially adenine and thymine in supramolecular adhesives have remarkable capacity for forming hydrogen bonds, metal-coordination bonds, π–π stacking and hydrophobic interactions.[39,40] More importantly, the specific hydrogen bonding between complementary nucleobases enables the elegant modulation of the adhesive properties.[20,40]

To fabricate strong supramolecular polymeric adhesives, optimizing the adhesive and cohesive properties is of great significance. However, it is highly challenging to achieve the balanced adhesion and cohesion. For example, high supramolecular crosslinking for supramolecular polymeric adhesives potentially gives rise to improved intermolecular cohesion. As a consequence, the lower exposed functional groups at the interface decrease the interfacial adhesion dramatically. Therefore, common strategies often enhance one property at the expense of another.[22,41] The key issue is attributed to that the supramolecular interactions for interfacial adhesion and intermolecular cohesion are highly coupled. Hence, developing a straightforward and feasible strategy to decouple interfacial adhesion and intermolecular cohesion is highly desired, potentially achieving the balanced adhesion and cohesion for enhanced properties and significantly expanding the applicability of supramolecular adhesives.

Herein, we have developed an efficient approach to enhance the adhesion strength without drastically destructing the intermolecular cohesion through the counterion exchange of polyelectrolytes (Fig. 1). The cationic polyelectrolyte poly(3-acrylamidopropyltrimethylammonium chloride) (PTMPA-Cl), which can undergo efficient counterion exchanges, was successfully prepared through free radical polymerization. After exchanging to sulfonates with different hydrophobic chain lengths, the slightly enhanced intermolecular cohesion of the polyelectrolyte improves the adhesion strength. To further reinforce the intermolecular cohesion, bioinspired complementary nucleobases were introduced. Unexpectedly, the loss of interfacial adhesion was observed for adhesives with high supramolecular hydrogen-bonding crosslinking densities. The cohesive and adhesive properties of nucleobase-containing polyelectrolyte adhesives can be balanced through counterion exchange, achieving 60 to 250 times improvement over that of initial supramolecular polymeric adhesives. More importantly, the robust nucleobase-containing supramolecular polymeric adhesives display outstanding tolerance to different external conditions, manifesting excellent applicable potentials. Therefore, this work provides an efficient method to fabricate robust and tunable supramolecular adhesives by balancing the cohesive and adhesive properties.

Results and discussion

Synthesis and properties of poly(3-acrylamidopropyltrimethylammonium chloride) (PTMPA-Cl) exchanged with different counterions

Poly(3-acrylamidopropyltrimethylammonium chloride) (PTMPA-Cl) as one of the typical cationic polyelectrolytes was prepared through conventional free radical polymerization in water at 70 °C (Scheme S1†). 2,2′-Azobis[2-(2-imidazolin-2-yl) propane] dihydrochloride (VA-044) was used as a water soluble initiator and high conversion (99%) was obtained after polymerization for 2 h. Size exclusion chromatography (SEC) analysis shows that PTMPA-Cl with a number-average molecular weight of 35.5 kDa and polydispersity ($Đ$) of 2.71 was yielded (Fig. S1†). We choose sodium methanesulfonate, sodium 1-butanesulfonate, and sodium 1-octanesulfonate, which have different lengths of hydrophobic chains for counterion exchanges. The PTMPA-Cl aqueous solution was mixed with aqueous solutions containing different sulfonates. The obtained mixtures were further dialyzed against water to yield the targeted product. PTMPA-C_1, PTMPA-C_4, and PTMPA-C_8 were obtained when the counterion of PTMPA-Cl was exchanged with sodium methanesulfonate, sodium 1-butanesulfonate, and sodium 1-octanesulfonate, respectively (Scheme S1†).

According to the Law of Matching Water Affinities (LMWA), the weakly hydrated quaternary ammonium groups attached to the polymer PTMPA-Cl are inclined to bind weakly to the chloride ion (Cl^-).[42–46] In contrast, stronger binding was formed between the weakly hydrated alkyl sulfonate anions and the quaternary ammonium groups.[42–46] The unique properties

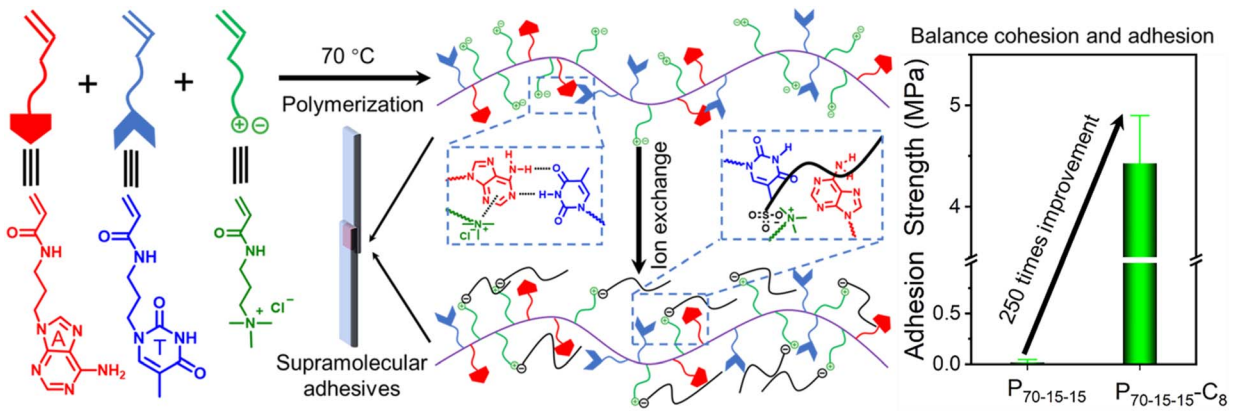

Fig. 1 Schematic diagram of the fabrication of nucleobase-containing supramolecular adhesives. The counterion exchange of positively charged polyelectrolytes enables us to enhance the adhesive properties by balancing cohesion and adhesion.

enable us to exchange the chloride counterion with different sulfonates. The successful exchange of counterions was confirmed by ^{1}H NMR spectra, FT-IR spectra, and surface wettability (Fig. 2a and S2, S3†). As shown in Fig. 2a, a significant shift of the peak at 3.22 ppm to 3.14 ppm was observed, which is assigned to protons in the alkyl group attached to the ammonium. Considering that the interaction between Cl^- and the ammonium group is different from that between the sulfonate and the ammonium group, the peak for protons in the alkyl group connected to the ammonium shifted to the high field in all PTMPA-C_1, PTMPA-C_4, and PTMPA-C_8. In addition, other new peaks for the sulfonates have emerged, suggesting the successful exchange of counterions (Fig. 2a). Furthermore, X-ray photoelectron spectroscopy (XPS) analyses show that the peak for Cl2p fully disappears and the peak for S2p emerges for PTMPA-C_1, PTMPA-C_4, and PTMPA-C_8 (Fig. S4†). These results have validated that the counterion exchange between Cl^- and the sulfonates is nearly complete.

Fig. 2b shows that the exchange of the counterions was further verified by DSC analyses. The polymer PTMPA-Cl has a glass transition temperature (T_g) of 82.5 °C, which was due to the rigid polymer chain of the polyelectrolyte. In stark contrast, T_gs of PTMPA-C_1 and PTMPA-C_4 were observed to decrease to −13.9 °C and −25.5 °C, respectively. Compared with PTMPA-Cl, the significant drop of T_g can be attributed to the efficient electrostatic shield owing to the stronger interaction between the sulfonate and the ammonium group. Intriguingly, PTMPA-C_8 presents a high T_g of 62.1 °C. For PTMPA-Cl, PTMPA-C_1, PTMPA-C_4, and PTMPA-C_8, they consist of the cationic polyelectrolyte poly(3-acrylamidopropyltrimethylammonium) with different counterions. As a result, the dominant intermolecular interaction is the hydrophobic interaction. We suppose that the hydrophobic interaction of the long alkyl chain in PTMPA-C_8 leads to the decrease of segment mobility. Further increase of the chain length of the counterion to 1-dodecanesulfonate gives a similar result, suggesting that the alkyl group with the carbon number as long as 8 is essential for the strong interaction (Fig. S5†). Additionally, all these polymers have good thermal stability with the decomposition temperature over 268 °C, demonstrating good application potential (Fig. S6†).

The adhesion strengths of PTMPA-Cl, PTMPA-C_1, PTMPA-C_4, and PTMPA-C_8 were evaluated through shear tests by using stainless steel as the substrate (Fig. 2c). A gradual increase of

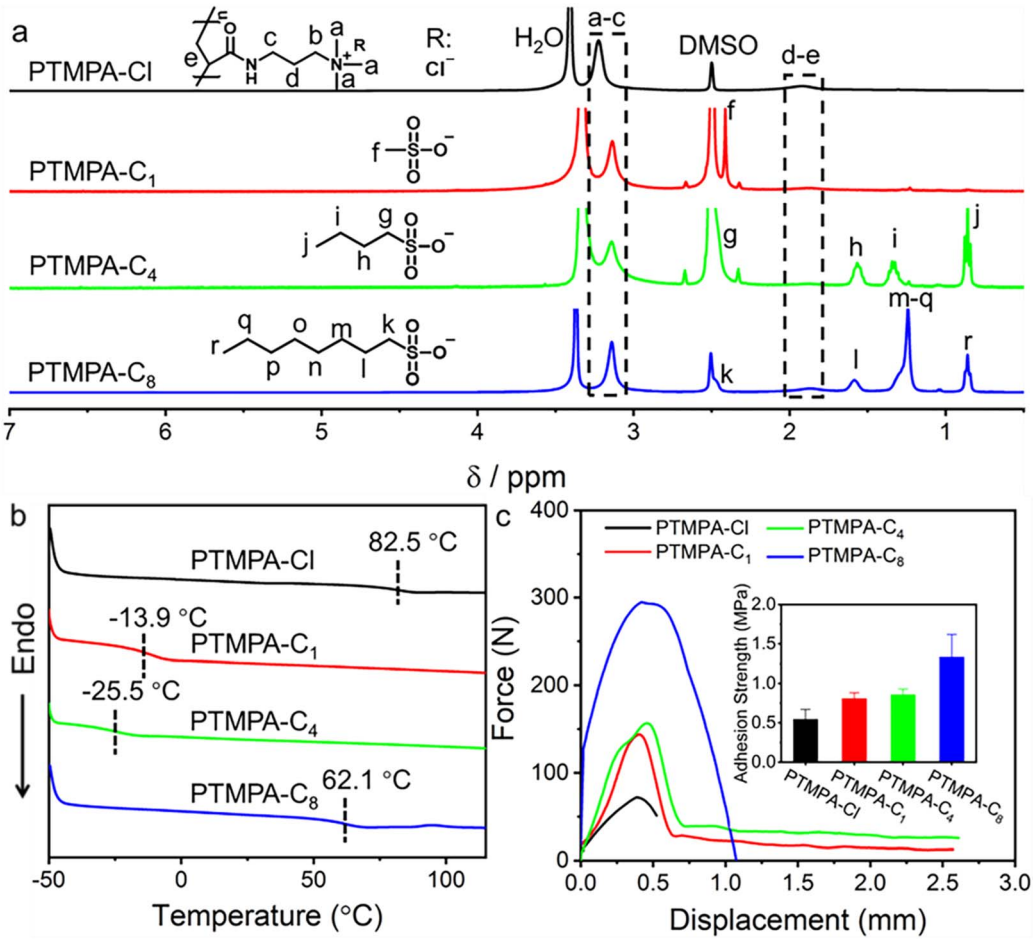

Fig. 2 Characterization of cationic PTMPAs with different counterions. (a) ^{1}H NMR spectra and (b) DSC curves of PTMPA-Cl, PTMPA-C_1, PTMPA-C_4, and PTMPA-C_8. (c) Representative shear test curves for PTMPA-Cl, PTMPA-C_1, PTMPA-C_4, and PTMPA-C_8 with the inset showing the adhesion strengths.

the maximum adhesive force was observed from 72 N for PTMPA-Cl to 295 N for PTMPA-C_8. The inset in Fig. 2c shows that the adhesion strength of PTMPA-Cl is 0.54 ± 0.12 MPa. Further, the adhesion strengths of PTMPA-C_1, PTMPA-C_4, and PTMPA-C_8 are observed to increase to 0.81 ± 0.07 MPa, 0.86 ± 0.07 MPa, and 1.33 ± 0.28 MPa, respectively. Although PTMPA-Cl is inclined to have strong interfacial adhesion with the substrate, the low intermolecular cohesion generates weak adhesion strength. After exchanging to the sulfonates, the intermolecular cohesion within PTMPA-C_1, PTMPA-C_4, and PTMPA-C_8 was enhanced through the additional hydrophobic interaction of counterions, resulting in the improvement of adhesive properties.

Syntheses and adhesive properties of nucleobase-containing polyelectrolytes

Since all the PTMPA polymers with different counterions undergo cohesive failures upon the shear test, the adhesion strengths of these polymers are expected to further be improved by increasing the intermolecular cohesion. A series of nucleobase-containing polyelectrolytes $P_{(100-2x,\ x,\ x)}$s were synthesized through the ternary copolymerization of 3-(adenine-9-yl) propyl acrylamide (AAm), 3-(thymin-1-yl) propyl acrylamide (TAm), and TMPA-Cl, in which x represents the molar percent ratio of nucleobase-containing monomers in the copolymers (Scheme S2† and Fig. S7 and S8†). ^{1}H NMR spectroscopy was used to obtain the final conversion of the nucleobase-containing copolymers by analysing the mixture after polymerization without purification (Fig. S9†). The integration of residual double bonds in the mixture suggests over 99% conversion of monomers was achieved for all $P_{90\text{-}5\text{-}5}$, $P_{80\text{-}10\text{-}10}$, and $P_{70\text{-}15\text{-}15}$. Both the adenine and thymine molar ratios in the copolymer can be obtained from the initial feeding and the monomer conversion. As shown in Fig. S9,† nearly full conversion of feeding monomers was observed for the ternary copolymers. Therefore, the final attained polymers are supposed to have the same molar percentage as the initial target. The intermolecular hydrogen bonding interaction between AAm and TAm is capable of forming supramolecular crosslinking, generating enhanced cohesion. Of note, when the molar percent ratios of AAm and TAm are over 20 mol%, high supramolecular crosslinking leads to the formation of hydrogels, hampering the purification and probable applications as supramolecular polymeric adhesives. Therefore, copolymers $P_{90\text{-}5\text{-}5}$, $P_{80\text{-}10\text{-}10}$, and $P_{70\text{-}15\text{-}15}$ were prepared and further investigated as supramolecular polymeric adhesives.

As shown in Fig. 3a, ^{1}H NMR spectra manifest the successful copolymerization of the three monomers. The peak at 3.21 ppm can be assigned to the methyl group appended to the

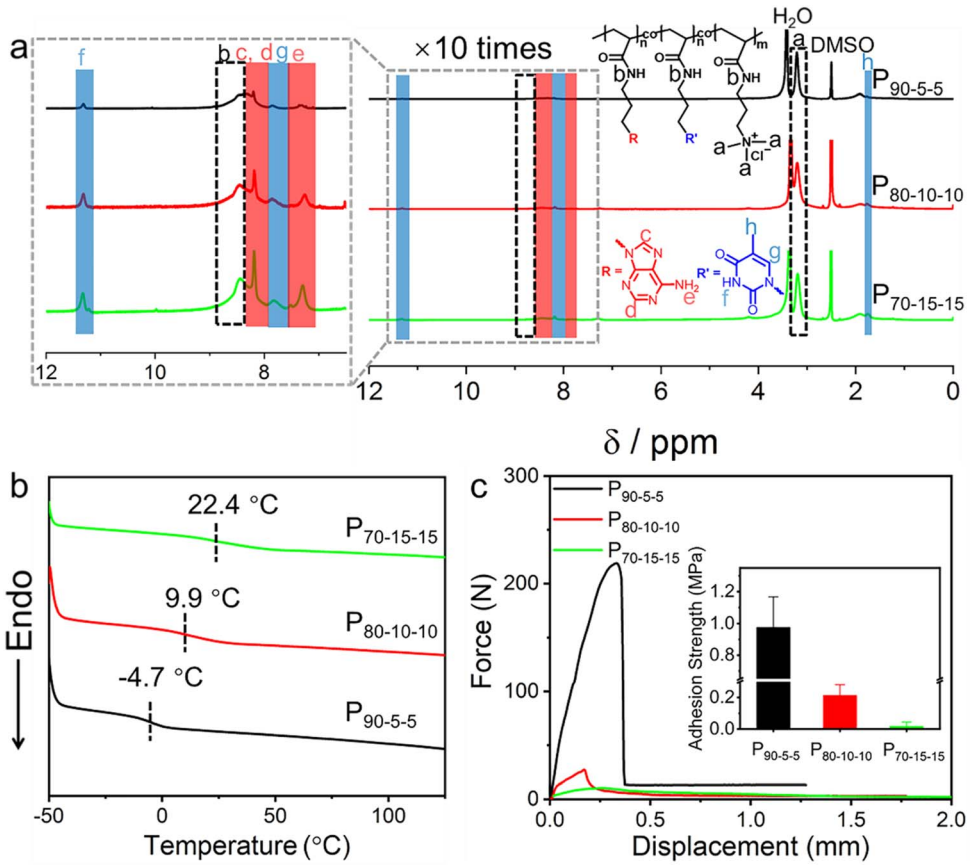

Fig. 3 Characterization of nucleobase-containing polyelectrolytes. (a) ^{1}H NMR spectra and (b) DSC curves of $P_{90\text{-}5\text{-}5}$, $P_{80\text{-}10\text{-}10}$, and $P_{70\text{-}15\text{-}15}$. (c) Representative shear test curves for $P_{90\text{-}5\text{-}5}$, $P_{80\text{-}10\text{-}10}$, and $P_{70\text{-}15\text{-}15}$ with the inset showing the adhesion strengths.

ammonium. Meanwhile, the peaks at 8.20 and 7.36 ppm are assigned to adenine and the peaks at 11.33 and 7.87 ppm are assigned to thymine. Obviously, the peaks for both adenine and thymine gradually increase as the contents of them are improved in the copolymers. DSC analyses show that a single T_g was observed for the copolymers $P_{90\text{-}5\text{-}5}$, $P_{80\text{-}10\text{-}10}$, and $P_{70\text{-}15\text{-}15}$, illustrating the random copolymerization of the comonomers (Fig. 3b). Interestingly, compared with PTMPA-Cl with a T_g of 82.5 °C, the T_g of $P_{90\text{-}5\text{-}5}$ is as low as −4.7 °C after introducing 10 mol% of nucleobase-containing monomers. In addition to the perturbation of electrostatic interaction in PTMPA-Cl, the cation–π interaction should play a dominant role in the copolymer. Both the purine and pyrimidine structures of nucleobases facilitate the formation of cation–π interactions, further decreasing the repulsion between different chain segments. Considering the increase of supramolecular crosslinking between complementary nucleobases, the T_gs of the copolymers were observed to present an increasing trend with the further increase of nucleobase-containing monomers (Fig. 3b). Additionally, all these nucleobase-containing polyelectrolytes have good thermal stability with the decomposition temperature over 264 °C, demonstrating good applicability (Fig. S10†).

Interestingly, the adhesion strengths of the nucleobase-containing polyelectrolytes show a dramatic decrease from 0.98 ± 0.19 MPa for $P_{90\text{-}5\text{-}5}$ to 0.21 ± 0.06 MPa for $P_{80\text{-}10\text{-}10}$ (inset in Fig. 3c). Further increase of nucleobase-containing moieties in the adhesive leads to the loss of efficient adhesion (18 ± 16 kPa). As expected, the introduction of nucleobases should be beneficial to the adhesion owing to the existence of functional aromatic groups. Indeed, a higher adhesion strength was observed for $P_{90\text{-}5\text{-}5}$, in contrast to the adhesion strength of 0.54 ± 0.12 MPa for PTMPA-Cl. Nonetheless, the formed hydrogen bonding and cation–π interactions cannot be neglected in the adhesives with high nucleobase contents, bringing about strong cohesion. As a result, the adhesives $P_{80\text{-}10\text{-}10}$ and $P_{70\text{-}15\text{-}15}$ have strong cohesion but weak interfacial adhesion, resulting in low adhesion strengths.

Enhanced adhesive properties of nucleobase-containing polyelectrolytes modulated through counterion exchange

For nucleobase-containing polyelectrolytes, the unbalanced cohesion and adhesion generate relatively weak adhesion strengths. Notably, the charged parts in nucleobase-containing polyelectrolytes provide an additional handle to modulate the cohesive and adhesive properties of adhesives, which might not interrupt the supramolecular hydrogen bonding. Therefore, the adhesive properties of nucleobase-containing polyelectrolytes can be boosted through counterion exchange (Scheme S2 and Fig. S11–S13†). Indeed, a gradual increase of the adhesion strengths was observed when the length of counterion alkyl chains was increased from 1 to 4, and then to 8 for all $P_{90\text{-}5\text{-}5}$, $P_{80\text{-}10\text{-}10}$, and $P_{70\text{-}15\text{-}15}$ (Fig. 4a). The adhesion strength of $P_{70\text{-}15\text{-}15}$-$C_8$ is as high as 4.43 ± 0.47 MPa, which is over 250 times higher than that of $P_{70\text{-}15\text{-}15}$. The bioinspired nucleobase-containing polyelectrolyte $P_{70\text{-}15\text{-}15}$-$C_8$ reported in this work outperforms most of the common PSAs, supramolecular adhesives, and epoxy resins (Fig. S14†). Meanwhile, the adhesion strength of the bioinspired nucleobase-containing polyelectrolyte is on par with the strong mussel-inspired adhesives, showing good potential applicability. Additionally, the adhesion strengths of both $P_{80\text{-}10\text{-}10}$-$C_8$ and $P_{80\text{-}10\text{-}10}$-$C_4$ also represent over 10 times enhancement over $P_{80\text{-}10\text{-}10}$. Hence, the counterion exchange provides a straightforward and feasible approach to alter the properties of adhesives over a wide range.

To further explore the enhanced adhesive properties of nucleobase-containing polyelectrolytes with different counterions, FT-IR and DSC analyses were utilized to unveil the underlying mechanism (Fig. 4b–e). FT-IR spectra display that new peaks at 1044 and 1085 cm^{-1} emerged after exchanging with different counterions for $P_{90\text{-}5\text{-}5}$ (Fig. 4b). These new peaks can be assigned to the vibration absorbance of the S=O bond. A slight shift from 1201 cm^{-1} for methanesulfonate to 1185 cm^{-1} for sulfonates with long alkyl chains was observed, illustrating the stronger interaction with the ammonium group for methanesulfonate than that for 1-butanesulfonate and 1-octanesulfonate. Meanwhile, no significant change of the absorbance at 1600 cm^{-1} was discerned, which was attributed to the bending vibration peak of N–H= involving the hydrogen bonding between complementary nucleobases.

DSC curves show that the $P_{90\text{-}5\text{-}5}$-C_1 and $P_{90\text{-}5\text{-}5}$-C_4 have T_g values of 29.5 and 26.2 °C, which are much higher than that of $P_{90\text{-}5\text{-}5}$ (Fig. 4c). Interestingly, $P_{90\text{-}5\text{-}5}$-C_8 has a lower T_g of −7.0 °C than that of $P_{90\text{-}5\text{-}5}$. Considering the low supramolecular crosslinking for $P_{90\text{-}5\text{-}5}$, the counterion exchange is unable to disturb the supramolecular hydrogen-bonding interaction, which was confirmed by FT-IR analyses (Fig. 4b). Additionally, the cation–π and hydrophobic interactions should play an important role in tuning the properties of the adhesives. The short alkyl chains of counterions in $P_{90\text{-}5\text{-}5}$-C_1 and $P_{90\text{-}5\text{-}5}$-C_4 did not influence the cation–π interactions dramatically, but the hydrophobic interaction was enhanced within the adhesives. Consequently, the T_gs of both $P_{90\text{-}5\text{-}5}$-C_1 and $P_{90\text{-}5\text{-}5}$-C_4 present a significant increase. In contrast, $P_{90\text{-}5\text{-}5}$-C_8 with a long alkyl chain can possibly disrupt the cation–π interaction, giving rise to a high chain mobility. Although the octane chain in $P_{90\text{-}5\text{-}5}$-C_8 might be able to form hydrophobic aggregation during the counterion exchange, the disruption of the cation–π interaction affects the chain mobility more dramatically. Taken together, the counterion exchange for $P_{90\text{-}5\text{-}5}$ did not significantly change the supramolecular hydrogen bonding related to cohesion. Yet, the disruption of cation–π interaction and the formation of hydrophobic interaction are able to enhance the interfacial adhesion. Similar phenomena were observed for $P_{80\text{-}10\text{-}10}$ with relatively low supramolecular crosslinking (Fig. S15 and S16†). Therefore, the adhesion strengths were improved for $P_{90\text{-}5\text{-}5}$ and $P_{80\text{-}10\text{-}10}$ after exchanging with the counterions by improving the adhesion without compromising the cohesion.

For $P_{70\text{-}15\text{-}15}$ with a high supramolecular crosslinking, FT-IR analyses show that the absorbance at 1600 cm^{-1} for the hydrogen bonding interaction was disrupted when exchanging with 1-octanesulfonate (Fig. 4d). In contrast to $P_{90\text{-}5\text{-}5}$ and $P_{80\text{-}10\text{-}10}$, the T_g of $P_{70\text{-}15\text{-}15}$ with different sulfonates presents a distinct

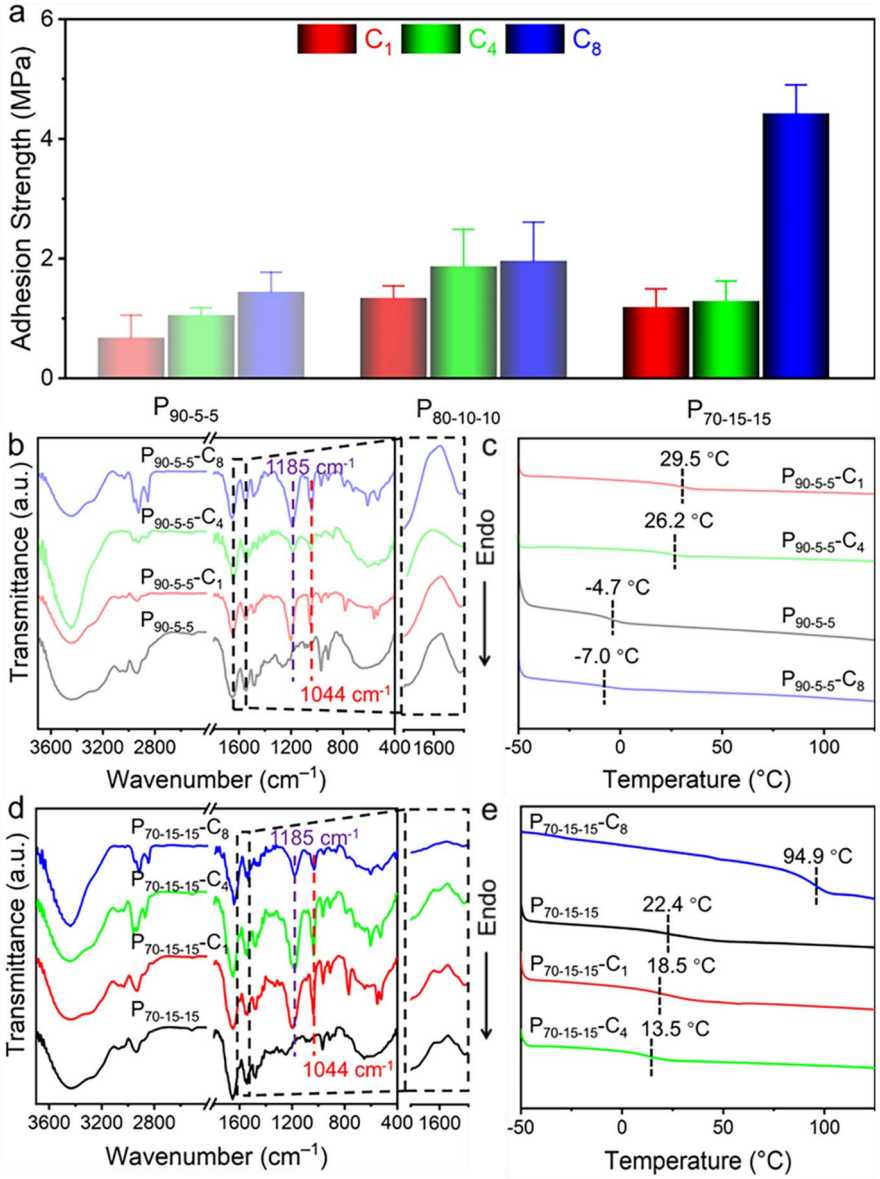

Fig. 4 Adhesion strengths of nucleobase-containing polyelectrolytes modulated through counterion exchange. (a) Adhesion strengths of $P_{90\text{-}5\text{-}5}$, $P_{80\text{-}10\text{-}10}$, and $P_{70\text{-}15\text{-}15}$ with different counterions. (b) FT-IR spectra and (c) DSC curves of $P_{90\text{-}5\text{-}5}$ with different counterions. (d) FT-IR spectra and (e) DSC curves of $P_{70\text{-}15\text{-}15}$ with different counterions.

trend. In addition to stronger supramolecular crosslinking, the higher nucleobase monomers and TMPA ratio in $P_{70\text{-}15\text{-}15}$ generate more efficient cation–π interaction. For $P_{70\text{-}15\text{-}15}$-$C_1$ and $P_{70\text{-}15\text{-}15}$-$C_4$, the weakened cation–π interaction by the exchanged counterions leads to a higher chain mobility. Interestingly, $P_{70\text{-}15\text{-}15}$-$C_8$ has a high T_g of 94.9 °C. This result should be caused by the weakened cation–π interaction and the significantly enhanced hydrophobic interactions between long alkyl chains and nucleobases. Notably, the disruption of complementary hydrogen bonding is vital for strong interfacial adhesion, which enables the exposure of nucleobase functionalities. As a result, $P_{70\text{-}15\text{-}15}$-$C_8$ is capable of achieving an ultrastrong adhesion strength by balancing the adhesion and cohesion interaction.

Robust adhesive properties of nucleobase-containing polyelectrolytes

The nucleobase-containing polyelectrolyte $P_{70\text{-}15\text{-}15}$-$C_8$ shows an adhesion strength of as high as 4.43 MPa with stainless steel as the substrate after having 1-octanesulfonate as the counterion. We wondered whether the robust adhesive properties are universal to different substrates. In addition to stainless steel, several substrates such as polyethylene (PE), polymethylmethacrylate (PMMA), quartz glass, and ceramics are also employed to investigate the adhesive properties (Fig. 5a). Low adhesion strengths of 0.18 MPa and 0.46 MPa were observed for PE and PMMA respectively, indicating the importance of electrostatic interaction for the efficient

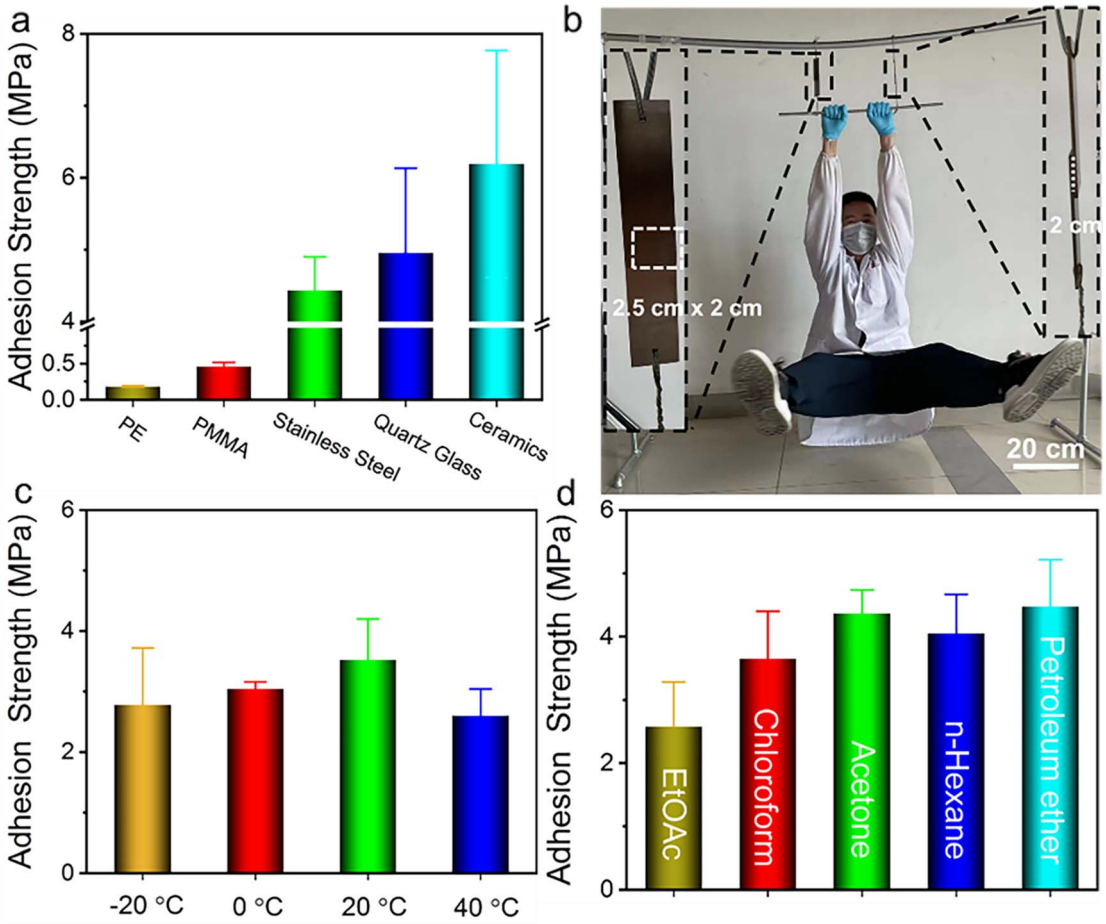

Fig. 5 Adhesive properties of the nucleobase-containing polyelectrolyte $P_{70\text{-}15\text{-}15}$-$C_8$. (a) Adhesion strengths of $P_{70\text{-}15\text{-}15}$-$C_8$ on different substrates including polyethylene (PE), polymethylmethacrylate (PMMA), stainless steel, quartz glass, and ceramics. (b) Demonstration of the robust adhesion strength of $P_{70\text{-}15\text{-}15}$-$C_8$ on the stainless steel by holding a person over 70 kg. The robust adhesion strength of $P_{70\text{-}15\text{-}15}$-$C_8$ for the stainless steel substrate (c) at different temperatures or (d) after immersed into different solvents for 2 h.

adhesion of positively charged polyelectrolyte adhesives. The polymeric substrates PE and PMMA hinder the formation of strong interfacial adhesion. In contrast, the adhesive $P_{70\text{-}15\text{-}15}$-$C_8$ is able to achieve strong adhesion for quartz glass and ceramics with adhesion strengths of 4.95 ± 1.18 MPa and 6.19 ± 1.58 MPa, considering the additional electrostatic interaction with the substrate. It is noted that the quartz glass bonded with $P_{70\text{-}15\text{-}15}$-$C_8$ cannot be separated prior to the breakage of the glass substrate with the contact area of 1.50 cm × 1.25 cm. Therefore, we utilized a small contact area of 0.50 cm × 0.50 cm for measuring the adhesion strength of glass substrates bonded with $P_{70\text{-}15\text{-}15}$-$C_8$ (Fig. S17†).

As shown in Fig. 5b a person with a weight over 70 kg can be easily held by two $P_{70\text{-}15\text{-}15}$-$C_8$ bonded steel substrates, demonstrating robust adhesion strength (Movie S1†). Meanwhile, the strongly adhesive $P_{70\text{-}15\text{-}15}$-$C_8$ shows good environmental tolerance towards different environmental conditions. High adhesion strengths over 2.60 MPa are observed for the adhesive $P_{70\text{-}15\text{-}15}$-$C_8$ from −20 °C to 40 °C, illustrating the widespread application temperature window (Fig. 5c). In addition, the adhesive presents good tolerance to different organic solvents such as ethyl acetate (EtOAc), chloroform, acetone, *n*-hexane, and petroleum ether. High adhesion strengths over 2.58 MPa were retained after immersing into the solvents for over 2 h (Fig. 5d). It is possible for highly polar solvents to swell the adhesive, inducing a decrease of adhesion strengths. More importantly, the supramolecular adhesive $P_{70\text{-}15\text{-}15}$-$C_8$ can be harnessed for repeated adhesion. No obvious decrease of the adhesion strength after several adhesion–shear–adhesion cycles was observed with the adhesion strength over 4.08 MPa continuously (Fig. S18†). Collectively, the nucleobase-containing polyelectrolyte adhesives have strong adhesive properties under distinct environmental conditions, showing tremendous applicability. Both adenine and thymine-containing polymers are confirmed to be biocompatible, and the cationic polyelectrolyte poly(3-acrylamidopropyltrimethylammonium chloride) is supposed to be biocompatible and antibacterial. Therefore, the strong adhesives developed in this work are potential biomedical adhesives for wound dressing or implantable biomedical devices.

Experimental

Materials

2,2′-Azobis[2-(2-imidazolin-2-yl) propane] dihydrochloride (VA-044) was obtained from Aladdin and recrystallized from methanol three times before use. *N*,*N*-Dimethylformamide (DMF, 99.9%) was purified by using a solvent purification system (MB-SPS-5) before use. 3-Acrylamidepropyl-trimethylammonium chloride (TMPA-Cl, 75 wt% in water) was purified by filtering through an alkaline alumina column to remove the polymerization inhibitor. The water used was purified by filtration through a Millipore Gradient system, giving a resistivity of 18.2 MΩ cm. Other chemicals were purchased from Aladdin and used directly without further purification. 3-(Adenine-9-yl) propyl acrylamide (AAm) and 3-(thymin-1-yl) propyl acrylamide (TAm) were prepared according to the previous publication.

Methods

All ^{1}H NMR spectra were recorded on an Avance III HD400 spectrometer (Bruker) with DMSO-d_6 as the solvent. Fourier transform infrared (FT-IR) spectra were obtained on a Nicolet 6700 spectrometer (Thermo Scientific). The molecular weight and molecular weight distribution of cationic polymer PTMPA-Cl and nucleobase-containing polymers were measured by size exclusion chromatography (SEC) at 20 °C with aqueous solution (100 mM NaCl, 25 mM NaH_2PO_4, and 25 mM Na_2HPO_4) as the eluent at a flow rate of 1 mL min^{-1}. SEC data were analysed with Agilent SEC software calibrated with PEO standards prior to use. Thermogravimetric analysis (TGA) was carried out on a TA Q5000IR TGA instrument under a nitrogen atmosphere to obtain the decomposition temperature ($T_{d,\ 5\%}$) at 5% degradation of the polymers. Polymers with a weight of about 5–10 mg were slowly heated up from 40 to 700 °C with a rate of 10 °C min^{-1} to explore the thermal stability. Glass transition temperatures (T_gs) of obtained polymers were characterized by differential scanning calorimetry (DSC) using a PerkinElmer DSC 8500 instrument under a nitrogen atmosphere. The dried sample was first heated from room temperature to 150 °C at a rate of 10 °C min^{-1}, and then cooled down to −50 °C at the same rate. Following this, the sample was reheated to 150 °C at a rate of 10 °C min^{-1}. The T_g value was attained from the second heating scan. For the adhesive test, the typical preparation process of the sample is as follows. The $P_{70\text{-}15\text{-}15}$-$C_8$ polymer was put on stainless steel (1.50 × 1.25 cm^2) at 80 °C on a heating plate. Then another piece of stainless steel sheet was pasted on it, and pressed on the stainless steel sheet with 500 g weight for 5 min. The bonded sample was placed in a vacuum oven at 60 °C for 24 h, and then the sample was kept at 25 °C and 50% RH for 8 h before the adhesion strength was tested. Although the sample preparation temperature is slightly lower than the T_g of $P_{70\text{-}15\text{-}15}$-$C_8$, enough heating and annealing time guarantees efficient interfacial wetting. Characterization of adhesive properties of nucleobase-containing adhesives with sulfonate ions of different alkyl chain lengths was performed on a SANS TS7104 electronic testing instrument (SANS, China) at 10 mm min^{-1}. Each polymer sample was measured at least five times to ensure repeatability. Based on the same procedures, the adhesion strengths were tested when bonding with different substrates, immersed into organic solvents and exposed under different temperatures. The water contact angle (WCA) was determined by using a contact angle goniometer (CAM 200, KSV). The surface chemical element components of PTMPA-Cl and PTMPAs with different counterions were analysed by using X-ray photoelectron spectroscopy (XPS, Kratos Axis supra+). The instrument was equipped with a monochromatic Al Kα radiation source at 1486.6 eV, which detected the characteristic binding energies relevant to each element of sample.

Synthetic procedures

Synthesis of (PTMPA-Cl). A dried ampoule was charged with TMPA-Cl (1.30 g, 4.84 mmol), VA-044 (15.7 mg, 0.05 mmol), and deionized water (3.7 mL) (Scheme S1†). The reaction mixture was degassed through 3 freeze–pump–thaw cycles, and then put in an oil bath at 70 °C for 2 h with constant stirring. After polymerization, an aliquot of the reaction mixture was taken and analysed by ^{1}H NMR spectroscopy to calculate the conversion. The residual solution was precipitated three times from cold isopropanol. The purified polymer was dried in a vacuum oven overnight at room temperature and further characterized by ^{1}H NMR spectroscopy, SEC, FT-IR, DSC, and TGA, respectively.

Preparation of PTMPAs with different sulfonate counterions. Preparation of the PTMPA with different counterions sulfonates is shown in Scheme S1.† The purified PTMPA-Cl (100 mg, 0.48 mmol) was added to deionized water (2 mL). Into the dissolved PTMPA-Cl aqueous solution, sodium methanesulfonate (280 mg, 2.42 mmol), sodium 1-butanesulfonate (380 mg, 2.42 mmol), and sodium 1-octane sulfonate (530 mg, 2.42 mmol) dissolved in deionized water (1 mL) were added dropwise, respectively. For the mixed solutions containing PTMPAs exchanged with sodium methanesulfonate and sodium 1-butanesulfonate, both PTMPA-C_1 and PTMPA-C_4 can be obtained by dialysis and lyophilization. For both sodium 1-octane sulfonate and sodium 1-dodecane sulfonate with long alkyl chains, the counteranion exchange of PTMPA-Cl results in the occurrence of phase separation directly. The obtained white solids were further rinsed three times with deionized water.

Syntheses of random copolymers of TMPA, AAm, and TAm with different molar ratios. Poly((3-acrylamidopropyl trimethylammonium chloride)-*co*-(3-(adenine-9-yl) propyl acrylamide)-*co*-(3-(thymin-1-yl) propyl acrylamide)) P(TMPA-*co*-AAm-*co*-TAm) copolymers were prepared by using conventional free radical polymerization with VA-044 as the initiator (Scheme S2†). A typical synthetic procedure is as follows. For P($TMPA_{0.7}$-*co*-$AAm_{0.15}$-*co*-$TAm_{0.15}$) ($P_{70\text{-}15\text{-}15}$), a dried ampoule was charged with TMPA (784.5 mg, 2.85 mmol), AAm (150.0 mg, 0.61 mmol), TAm (144.5 mg, 0.61 mmol), VA-044 (13.1 mg, 0.04 mmol), and deionized water (3.5 mL). The reaction mixture was degassed through 3 freeze–pump–thaw cycles, and then put in an oil bath at 70 °C for 2 h with constant stirring. After

polymerization, an aliquot of the reaction mixture was taken and analysed by ^{1}H NMR spectroscopy to calculate the monomer conversion. The residual solution was precipitated three times from cold isopropanol. The purified polymer was dried in a vacuum oven overnight at room temperature and further characterized by ^{1}H NMR spectroscopy, SEC, FT-IR, DSC, and TGA, respectively.

Conclusions

In summary, bioinspired nucleobase-containing cationic polyelectrolytes can be harnessed as robust adhesives by balancing the interfacial adhesion and intermolecular cohesion through counterion exchange. First, it is found that the cationic polyelectrolyte PTMPA-Cl prepared through free radical polymerization can be effectively exchanged with different sulfonates. The enhanced intermolecular cohesion provides the polyelectrolytes containing different counterions with improved adhesion strengths. The cohesive failure for the polyelectrolyte adhesive prompts us to fabricate nucleobase-containing polyelectrolytes with high supramolecular crosslinking for robust adhesive behaviors. Interestingly, the dense supramolecular hydrogen-bonding crosslinking in the adhesive gives rise to the loss of interfacial adhesion. Further counterion exchange of the nucleobase-containing polyelectrolytes enables the boost of interfacial adhesion without significantly compromising the intermolecular cohesion. By balancing the cohesive and adhesive properties through counterion exchange, the adhesion strengths of nucleobase-containing polyelectrolytes can be improved as high as 250 times. In addition, the nucleobase-containing supramolecular polymeric adhesive manifests strong adhesion to distinct inorganic substrates. Meanwhile, the robust adhesive can tolerate the dramatic change of temperatures and various organic solvents, showcasing tremendous potential applicability. This work reports an efficient route for modulating the properties of supramolecular polymeric adhesives by achieving balanced adhesion and cohesion.

Data availability

The data that support the findings of this study are available from the corresponding author upon reasonable request.

Author contributions

The manuscript was written through contributions of all authors. All authors have given approval to the final version of the manuscript. Z. H. and G. L. conceived the study. Z. D. and J. W. carried out most of the experiments and analyzed the related data. X. S. participated in the experiments for monomers and polymer syntheses.

Conflicts of interest

The authors declare no competing financial interest.

Acknowledgements

This work was financially supported by the National Natural Science Foundation of China (22273098, 22103002, 52033001, and 21873091), Anhui Province Natural Science Funds (2008085QE249), the Fundamental Research Funds for the Central Universities (WK2480000007), and Anhui Provincial Innovation and Entrepreneurship Support Plan for Overseas Returnees (2019LCX023).

References

1 C. Ghobril and M. W. Grinstaff, The chemistry and engineering of polymeric hydrogel adhesives for wound closure: a tutorial, *Chem. Soc. Rev.*, 2015, **44**, 1820–1835.
2 C. Cui and W. Liu, Recent advances in wet adhesives: Adhesion mechanism, design principle and applications, *Prog. Polym. Sci.*, 2021, **116**, 101388.
3 M. Chen, Y. Wu, B. Chen, A. M. Tucker, A. Jagota and S. Yang, Fast, strong, and reversible adhesives with dynamic covalent bonds for potential use in wound dressing, *Proc. Natl. Acad. Sci. U. S. A.*, 2022, **119**, e2203074119.
4 S. Rose, A. Prevoteau, P. Elzière, D. Hourdet, A. Marcellan and L. Leibler, Nanoparticle solutions as adhesives for gels and biological tissues, *Nature*, 2014, **505**, 382–385.
5 J. Sun, L. Xiao, B. Li, K. Zhao, Z. Wang, Y. Zhou, C. Ma, J. Li, H. Zhang, A. Herrmann and K. Liu, Genetically engineered polypeptide adhesive coacervates for surgical applications, *Angew. Chem., Int. Ed.*, 2021, **60**, 23687–23694.
6 L. Zhang, M. Liu, Y. Zhang and R. Pei, Recent Progress of Highly Adhesive Hydrogels as Wound Dressings, *Biomacromolecules*, 2020, **21**, 3966–3983.
7 S. M. Lim, J. Ryu, E. H. Sohn, S. G. Lee, I. J. Park, J. Hong and H. S. Kang, Flexible, Elastic, and Superhydrophobic/Superoleophilic Adhesive for Reusable and Durable Water/Oil Separation Coating, *ACS Appl. Mater. Interfaces*, 2022, **14**, 10825–10835.
8 D. Ratna, Modification of epoxy resins for improvement of adhesion: a critical review, *J. Adhes. Sci. Technol.*, 2003, **17**, 1655–1668.
9 D. W. R. Balkenende, R. A. Olson, S. Balog, C. Weder and L. Montero de Espinosa, Epoxy Resin-Inspired Reconfigurable Supramolecular Networks, *Macromolecules*, 2016, **49**, 7877–7885.
10 M. A. Droesbeke, R. Aksakal, A. Simula, J. M. Asua and F. E. Du Prez, Biobased acrylic pressure-sensitive adhesives, *Prog. Polym. Sci.*, 2021, **117**, 101396.
11 Q. Wang, W. B. Griffith, M. Einsla, S. Zhang, M. L. Pacholski and K. R. Shull, Bulk and Interfacial Contributions to the Adhesion of Acrylic Emulsion-Based Pressure-Sensitive Adhesives, *Macromolecules*, 2020, **53**, 6975–6983.
12 S. Noppalit, A. Simula, L. Billon and J. M. Asua, Paving the Way to Sustainable Waterborne Pressure-Sensitive Adhesives Using Terpene-Based Triblock Copolymers, *ACS Sustainable Chem. Eng.*, 2019, **7**, 17990–17998.
13 J. Li, S. Luo, F. Li and S. Dong, Supramolecular Polymeric Pressure-Sensitive Adhesive That Can Be Directly Operated

at Low Temperatures, *ACS Appl. Mater. Interfaces*, 2022, **14**, 27476–27483.

14 S. Chen, Z. Li, Y. Wu, N. Mahmood, F. Lortie, J. Bernard, W. H. Binder and J. Zhu, Hydrogen-Bonded Supramolecular Polymer Adhesives: Straightforward Synthesis and Strong Substrate Interaction, *Angew. Chem., Int. Ed.*, 2022, **61**, e202203876.

15 Q. Zhang, T. Li, A. Duan, S. Dong, W. Zhao and P. J. Stang, Formation of a Supramolecular Polymeric Adhesive via Water-Participant Hydrogen Bond Formation, *J. Am. Chem. Soc.*, 2019, **141**, 8058–8063.

16 H. Liu, S. Qin, J. Liu, C. Zhou, Y. Zhu, Y. Yuan, D. a. Fu, Q. Lv, Y. Song, M. Zou, Z. Wang and L. Wang, Bio-Inspired Self-Hydrophobized Sericin Adhesive with Tough Underwater Adhesion Enables Wound Healing and Fluid Leakage Sealing, *Adv. Funct. Mater.*, 2022, **32**, 2201108.

17 L. Liu, Z. Liu, Y. Ren, X. Zou, W. Peng, W. Li, Y. Wu, S. Zheng, X. Wang and F. Yan, A Superstrong and Reversible Ionic Crystal-based Adhesive Inspired by Ice Adhesion, *Angew. Chem., Int. Ed.*, 2021, **60**, 8948–8959.

18 X. Ji, M. Ahmed, L. Long, N. M. Khashab, F. Huang and J. L. Sessler, Adhesive supramolecular polymeric materials constructed from macrocycle-based host–guest interactions, *Chem. Soc. Rev.*, 2019, **48**, 2682–2697.

19 C. Heinzmann, C. Weder and L. M. de Espinosa, Supramolecular Polymer Adhesives: Advanced Materials Inspired by Nature, *Chem. Soc. Rev.*, 2016, **45**, 342–358.

20 Y. Tian, J. Wu, X. Fang, L. Guan, N. Yao, G. Yang, Z. Wang, Z. Hua and G. Liu, Rational Design of Bioinspired Nucleobase-Containing Polymers as Tough Bioplastics and Ultra-Strong Adhesives, *Adv. Funct. Mater.*, 2022, **32**, 2112741.

21 A. H. Hofman, I. A. van Hees, J. Yang and M. Kamperman, Bioinspired underwater adhesives by using the supramolecular toolbox, *Adv. Mater.*, 2018, **30**, 1704640.

22 B. D. B. Tiu, P. Delparastan, M. R. Ney, M. Gerst and P. B. Messersmith, Enhanced Adhesion and Cohesion of Bioinspired Dry/Wet Pressure-Sensitive Adhesives, *ACS Appl. Mater. Interfaces*, 2019, **11**, 28296–28306.

23 D. Pei, S. Yu, P. Liu, Y. Wu, X. Zhang, Y. Chen, M. Li and C. Li, Reversible Wet-Adhesive and Self-Healing Conductive Composite Elastomer of Liquid Metal, *Adv. Funct. Mater.*, 2022, **32**, 2204257.

24 O. Berger, C. Battistella, Y. Chen, J. Oktawiec, Z. E. Siwicka, D. Tullman-Ercek, M. Wang and N. C. Gianneschi, Mussel Adhesive-Inspired Proteomimetic Polymer, *J. Am. Chem. Soc.*, 2022, **144**, 4383–4392.

25 Y. Wang, G. Xia, H. Yu, B. Qian, Y. H. Cheung, L. H. Wong and J. H. Xin, Mussel-Inspired Design of a Self-Adhesive Agent for Durable Moisture Management and Bacterial Inhibition on PET Fabric, *Adv. Mater.*, 2021, **33**, 2100140.

26 Q. Lin, D. Gourdon, C. J. Sun, N. Holten-Andersen, T. H. Anderson, J. H. Waite and J. N. Israelachvili, Adhesion mechanisms of the mussel foot proteins mfp-1 and mfp-3, *Proc. Natl. Acad. Sci. U. S. A.*, 2007, **104**, 3782–3786.

27 H. Lee, N. F. Scherer and P. B. Messersmith, Single-molecule mechanics of mussel adhesion, *Proc. Natl. Acad. Sci. U. S. A.*, 2006, **103**, 12999–13003.

28 B. D. B. Tiu, P. Delparastan, M. R. Ney, M. Gerst and P. B. Messersmith, Cooperativity of Catechols and Amines in High-Performance Dry/Wet Adhesives, *Angew. Chem., Int. Ed.*, 2020, **59**, 16616–16624.

29 S. Das, G. Vasilyev, P. Martin and E. Zussman, Bioinspired Cationic-Aromatic Copolymer for Strong and Reversible Underwater Adhesion, *ACS Appl. Mater. Interfaces*, 2022, **14**, 26287–26294.

30 G. P. Maier, M. V. Rapp, J. H. Waite, J. N. Israelachvili and A. Butler, Adaptive synergy between catechol and lysine promotes wet adhesion by surface salt displacement, *Science*, 2015, **349**, 628–632.

31 W. Wei, L. Petrone, Y. Tan, H. Cai, J. N. Israelachvili, A. Miserez and J. H. Waite, An Underwater Surface-Drying Peptide Inspired by a Mussel Adhesive Protein, *Adv. Funct. Mater.*, 2016, **26**, 3496–3507.

32 J. Li, Z. Wang, Z. Hua and C. Tang, Supramolecular Nucleobase-Functionalized Polymers: Synthesis and Potential Biological Applications, *J. Mater. Chem. B*, 2020, **8**, 1576–1588.

33 W. Wang, S. Liu, B. Chen, X. Yan, S. Li, X. Ma and X. Yu, DNA-Inspired Adhesive Hydrogels Based on the Biodegradable Polyphosphoesters Tackified by a Nucleobase, *Biomacromolecules*, 2019, **20**, 3672–3683.

34 X. Liu, Q. Zhang, L. Duan and G. Gao, Tough adhesion of nucleobase-tackifed gels in diverse solvents, *Adv. Funct. Mater.*, 2019, **29**, 1900450.

35 X. Liu, Q. Zhang and G. Gao, Bioinspired Adhesive Hydrogels Tackified by Nucleobases, *Adv. Funct. Mater.*, 2017, **27**, 1703132.

36 J. Wu, H. Lei, J. Li, Z. Zhang, G. Zhu, G. Yang, Z. Wang and Z. Hua, Nucleobase-Tackified Renewable Plant Oil-Based Supramolecular Adhesives with Robust Properties Both under Ambient Conditions and Underwater, *Chem. Eng. J.*, 2021, **405**, 126976.

37 X. Liu, Q. Zhang, L. Duan and G. Gao, Bioinspired nucleobase-driven nonswellable adhesive and tough gel with excellent underwater adhesion, *ACS Appl. Mater. Interfaces*, 2019, **11**, 6644–6651.

38 S. Cheng, M. Zhang, N. Dixit, R. B. Moore and T. E. Long, Nucleobase Self-Assembly in Supramolecular Adhesives, *Macromolecules*, 2012, **45**, 805–812.

39 X. Liu, Q. Zhang, Z. Gao, R. Hou and G. Gao, Bioinspired adhesive hydrogel driven by adenine and thymine, *ACS Appl. Mater. Interfaces*, 2017, **9**, 17645–17652.

40 J. Wu, H. Lei, X. Fang, B. Wang, G. Yang, R. K. O'Reilly, Z. Wang, Z. Hua and G. Liu, Instant Strong and Responsive Underwater Adhesion Manifested by Bioinspired Supramolecular Polymeric Adhesives, *Macromolecules*, 2022, **55**, 2003–2013.

41 A. L. Dobson, N. J. Bongiardina and C. N. Bowman, Combined Dynamic Network and Filler Interface Approach for Improved Adhesion and Toughness in Pressure-

Sensitive Adhesives, *ACS Appl. Polym. Mater.*, 2020, **2**, 1053–1060.

42 K. D. Collins, Ions from the Hofmeister series and osmolytes: effects on proteins in solution and in the crystallization process, *Methods*, 2004, **34**, 300–311.

43 N. Vlachy, B. Jagoda-Cwiklik, R. Vacha, D. Touraud, P. Jungwirth and W. Kunz, Hofmeister series and specific interactions of charged headgroups with aqueous ions, *Adv. Colloid Interface Sci.*, 2009, **146**, 42–47.

44 L. Liu, R. Kou and G. Liu, Ion specificities of artificial macromolecules, *Soft Matter*, 2016, **13**, 68–80.

45 G. Liu, Tuning the Properties of Charged Polymers at the Solid/Liquid Interface with Ions, *Langmuir*, 2019, **35**, 3232–3247.

46 H. Yuan and G. Liu, Ionic effects on synthetic polymers: from solutions to brushes and gels, *Soft Matter*, 2020, **16**, 4087–4104.